Atmos. Meas. Tech., 9, 5509–5522, 2016
www.atmos-meas-tech.net/9/5509/2016/
doi:10.5194/amt-9-5509-2016

Atmospheric Measurement Techniques
Open Access
EGU

Comparison of two closed-path cavity-based spectrometers for measuring air–water CO_2 and CH_4 fluxes by eddy covariance

Mingxi Yang[1], John Prytherch[2], Elena Kozlova[3], Margaret J. Yelland[4], Deepulal Parenkat Mony[5], and Thomas G. Bell[1]

[1]Plymouth Marine Laboratory, Prospect Place, Plymouth, UK
[2]Institute for Climate and Atmospheric Science, School of Earth and Environment, University of Leeds, Leeds, UK
[3]College of Life and Environmental Sciences, University of Exeter, North Park Road, Exeter, UK
[4]National Oceanography Centre, European Way, Southampton, UK
[5]Inter University Centre for Development of Marine Biotechnology, School of Marine Sciences, Cochin University of Science and Technology, Cochin, India

Correspondence to: Mingxi Yang (miya@pml.ac.uk)

Received: 27 June 2016 – Published in Atmos. Meas. Tech. Discuss.: 24 August 2016
Revised: 27 October 2016 – Accepted: 2 November 2016 – Published: 18 November 2016

Abstract. In recent years several commercialised closed-path cavity-based spectroscopic instruments designed for eddy covariance flux measurements of carbon dioxide (CO_2), methane (CH_4), and water vapour (H_2O) have become available. Here we compare the performance of two leading models – the Picarro G2311-f and the Los Gatos Research (LGR) Fast Greenhouse Gas Analyzer (FGGA) at a coastal site. Both instruments can compute dry mixing ratios of CO_2 and CH_4 based on concurrently measured H_2O, temperature, and pressure. Additionally, we used a high throughput Nafion dryer to physically remove H_2O from the Picarro airstream. Observed air–sea CO_2 and CH_4 fluxes from these two analysers, averaging about 12 and 0.12 mmol m^{-2} day^{-1} respectively, agree within the measurement uncertainties. For the purpose of quantifying dry CO_2 and CH_4 fluxes downstream of a long inlet, the numerical H_2O corrections appear to be reasonably effective and lead to results that are comparable to physical removal of H_2O with a Nafion dryer in the mean. We estimate the high-frequency attenuation of fluxes in our closed-path set-up, which was relatively small (≤ 10 %) for CO_2 and CH_4 but very large for the more polar H_2O. The Picarro showed significantly lower noise and flux detection limits than the LGR. The hourly flux detection limit for the Picarro was about 2 mmol m^{-2} day^{-1} for CO_2 and 0.02 mmol m^{-2} day^{-1} for CH_4. For the LGR these detection limits were about 8 and 0.05 mmol m^{-2} day^{-1}. Using global maps of monthly mean air–sea CO_2 flux as reference, we estimate that the Picarro and LGR can resolve hourly CO_2 fluxes from roughly 40 and 4 % of the world's oceans respectively. Averaging over longer timescales would be required in regions with smaller fluxes. Hourly flux detection limits of CH_4 from both instruments are generally higher than the expected emissions from the open ocean, though the signal to noise of this measurement may improve closer to the coast.

1 Introduction

Eddy covariance is a direct and non-intrusive method for quantifying the vertical transport of carbon dioxide (CO_2) and methane (CH_4). This micro-meteorological technique derives fluxes from rapid fluctuations in the atmospheric CO_2 and CH_4 and thus requires a high-frequency (typically 10 Hz) chemical sensor. Over the last couple of decades, open path infrared gas analysers (IRGAs), such as the LI7500 (LI-COR Biosciences, Lincoln, Nebraska, USA), have been widely used to measure the atmosphere–biosphere as well as atmosphere–ocean exchange of CO_2. A similar instrument (LI7700) is available for measurements of CH_4 flux. The advantages of open-path sensors include small size, low power consumption, minimal lag time between chemical and wind

sensors, and no high-frequency signal attenuation from the inlet tube.

Miller et al. (2010), Blomquist et al. (2014), and Landwehr et al. (2014) demonstrated that air–sea CO_2 fluxes measured by LI7500s are subject to substantial biases due to variations in water vapour (H_2O). When measuring air–sea CO_2 fluxes, which are typically of the order of a few mmol m^{-2} day^{-1}, bias in the measured CO_2 fluxes due to H_2O can be 1 to 2 orders of magnitude greater than the actual CO_2 flux signal. This measurement bias is not related to the application of the air density correction (i.e. Webb et al., 1980); rather, it seems to be caused by cross-sensitivities between CO_2 and H_2O in the forms of spectral interference and pressure broadening (Kondo et al., 2014). The low-flux magnitude of CO_2 over the ocean and high humidity exacerbate this measurement bias. Furthermore, there appears to be little consistency even within the LI-COR family of products, with the LI7500 and the more recent LI7200 showing opposite signs in the H_2O bias (Landwehr et al., 2014). Uncertainties and nonlinearity in these cross-sensitivities complicate any mathematical corrections that try to address them (e.g. Prytherch et al., 2010; Edson et al., 2011). Miller et al. (2010) first showed that by converting the open path LI7500 to a closed-path configuration and physically drying the sampled air with a Nafion dryer, the accuracy and precision of the covariance CO_2 flux is significantly improved. The benefit of removing H_2O from the sampled air when measuring air–sea CO_2 fluxes with IRGAs was rigorously and quantitatively confirmed by Blomquist et al. (2014) and Landwehr et al. (2014).

In more recent years, cavity ring-down spectroscopy (CRDS; O'Keefe and Deacon, 1988) as well as off-axis integrated-cavity output spectroscopy (OA-ICOS; O'Keefe et al., 1999) have been developed and commercialised to measure CO_2 and CH_4. Two of the leading manufacturers are Picarro Inc., Santa Clara, California, USA (CRDS) and Los Gatos Research (LGR), Mountain View, California, USA (OA-ICOS). These instruments regulate the cavity (i.e. measurement cell) temperature and pressure, obviating the parts of the Webb et al. (1980) correction that are caused by fluctuations in air temperature and pressure. Blomquist et al. (2014) coupled a prototype Picarro CRDS instrument (G1301-f) to a Nafion dryer and measured CO_2 fluxes with an order of magnitude better precision (and free from H_2O bias) compared to measurements with open-path IRGAs (see more details in Sect. 3.2).

The latest models from Picarro (G2311-f) and LGR (enhanced performance Fast Greenhouse Gas Analyzer, FGGA) measure CO_2, CH_4, H_2O, as well as temperature and pressure simultaneously at 10 Hz. Observed H_2O mixing ratio is used to numerically correct on a point-by-point basis for the effect of humidity on the CO_2 and CH_4 signals by the instruments' internal software. This in theory enables the derivation of dry CO_2 and CH_4 fluxes without the need for a physical dryer (e.g. Nafion). The LGR FGGA is a fairly recent instrument and we are not aware of any published eddy covariance CO_2 or CH_4 fluxes using this instrument at sea. To the best of our knowledge, measurements of air–water fluxes Picarro and the LGR analysers have never been compared side by side.

Previous tests over terrestrial regions of very high fluxes are briefly reviewed here but do not provide sufficient information with respect to the suitability (or preference) of the Picarro and LGR instruments for air–sea flux measurements. Peltola et al. (2014) compared the performance of eight different instruments for eddy covariance CH_4 flux measurements over grassland, including the Picarro G2311-f and the LGR FGGA. They relied on the numerical H_2O corrections from the Picarro and the LGR instruments for the CH_4 flux calculations and did not look at the effect of using a Nafion dryer. The authors found that, in this environment with a typical CH_4 emission of the order of 2 mmol m^{-2} day^{-1}, cumulative measured fluxes from the G2311-f and the FGGA over 14 days agreed within 3 % (~ 0.8 mmol m^{-2}). Tuzson et al. (2010) found good agreement between an earlier-generation LGR instrument (with numerical H_2O correction) and a quantum cascade laser-based absorption spectrometer (physically dried) when measuring artificially generated CH_4 fluxes (> 1 mmol m^{-2} day^{-1}) by eddy covariance. In contrast to these areas of high fluxes, estimated CH_4 emissions over the open ocean are of the order of 0.01 mmol m^{-2} day^{-1} (e.g. Bange, 2006; Forster et al., 2009), placing greater demand on instrument accuracy and precision.

In this work, we compare the performance of the Picarro G2311-f and the LGR enhanced performance FGGA at measuring air–water fluxes of CO_2 and CH_4 by eddy covariance. Measurements were made from a coastal site, free from platform motion that might interfere with the flux signal (e.g. on ships or buoys, Prytherch et al., 2015). We compare the precision and flux detection limits of the two analysers, quantify the effects of H_2O fluctuations on the measured CO_2 and CH_4 fluxes, and examine the necessity of drying sample air when using these cavity-based instruments downstream of a long inlet. The gas flow rate required by the Picarro is fairly low (owing to the small cavity size), enabling efficient physical removal of water vapour from the sampled air with a dryer. The LGR has a much larger cavity cell that requires a higher gas flow to minimise high-frequency flux attenuation. The high flow rate results in decreased dryer performance and the LGR was thus configured without a dryer.

2 Experiment

2.1 Instrumental set-up

The Picarro G2311-f and the LGR FGGA were deployed side by side between 25 September and 2 October 2015 at the Penlee Point Atmospheric Observatory (PPAO; Fig. 1) on the south-west coast of the United Kingdom. Yang et al. (2016) provided detailed descriptions of this site and reported air–

sea CO_2 and CH_4 flux measurements from the open water wind sector (i.e. south-west) during spring/summer 2014–2015 using the Picarro G2311-f. During the week-long intercomparison described here, wind direction was predominantly from the north-east (Fig. A1) over the Plymouth Sound with a wind fetch over water of 5–6 km. Within this wind sector, measured momentum and sensible heat flux suggest that the flux footprint was also over the water only (Appendix, Figs. A2 and A3).

Both analysers sampled from the same ∼ 18 m long PFA inlet tube (1/4″ inner diameter), which led from inside the observatory to a sonic anemometer (Gill Windmaster Pro) on a retractable mast above the rooftop (∼ 18 m, a.s.l., above mean sea level). The gas inlet tip was about 30 cm below the sonic anemometer centre volume. A small, stainless steel particle filter (2 µm pore size, Swagelok SS-6F-05) was installed inline to protect the gas sensors from sea salt. An external scroll pump (BOC Edwards XDS-35i) was adjusted to pull ∼ 20 SLPM of air through the inlet tubing (measured by a mass flow meter). About ∼ 15 SLPM went through the cavity of the LGR analyser, which has a volume of 408 mL. The LGR cavity pressure was held at ∼ 140 Torr (0.184 atmosphere), resulting in a volumetric flow through the cavity of $\sim 80\,\mathrm{L\,min^{-1}}$. At this rate, the flushing time through the LGR cavity was 0.3 s.

The Picarro analyser subsampled from the main tubing ahead of the LGR at a flow rate of approximately $5\,\mathrm{L\,min^{-1}}$ (at atmospheric pressure). Maintained at a pressure of 153 Torr (0.20 atmosphere), the cavity volume of the Picarro (35 mL) is about 10 times smaller than that of the LGR. The flushing time in the cavity is thus less than 0.1 s and the manufacturer's stated response time is 0.2 s or less. Between 25 September and 1 October, a high throughput dryer (Nafion PD-200T-24M) was installed immediately upstream of the Picarro instrument (i.e. not affecting the LGR). The dryer was set up in the reflux configuration, utilising the reduced pressure of the Picarro exhaust air to dry the sample air. Using the LGR as reference, the dryer eliminated ∼ 80 % of H_2O (and ∼ 95 % of the rapid fluctuations in H_2O) in the sample stream of the Picarro instrument. We will refer to this sample period as Picarro (dry) vs. LGR (wet). Between 1 and 2 October, the Nafion dryer was removed in order to briefly examine the humidity dependence in the Picarro analyser. We will refer to this period as Picarro (wet) vs. LGR (wet).

2.2 Numerical corrections for water vapour

Both analysers report ambient mixing ratios of CO_2 and CH_4 (C_{CO_2} and C_{CH_4}) in parts per million (ppm). They compute the "dry mixing ratios" ($C_{CO_2\_d}$ and $C_{CH_4\_d}$, in ppm) based on the measured volume fraction of water vapour (C_{H_2O}, in %). Water vapour affects CO_2 and CH_4 measurements in cavity-based instruments in at least two ways: volumetric dilution and spectroscopic line broadening. Rella (2010) proposed the following corrections to account for both effects together:

$$C_{CO_2} = C_{CO_2\_d}(1 + aC_{H_2O} + bC_{H_2O}^2) \quad (1)$$

$$C_{CH_4} = C_{CH_4\_d}(1 + cC_{H_2O} + dC_{H_2O}^2). \quad (2)$$

For the Picarro G-2311f analyser, Chen et al. (2010) found $a = -0.01200$, $b = -2.674 \times 10^{-4}$, $c = -0.00982$, $d = -2.393 \times 10^{-4}$. When air is dried with a Nafion dryer, the reliance of the Picarro on these numerical corrections is reduced by about an order of magnitude. Different coefficients have been estimated for the LGR FGGA (Hiller et al., 2012). However, simple calculations using C_{CO_2}, $C_{CO_2\_d}$, C_{CH_4}, $C_{CH_4\_d}$, and C_{H_2O} in our observations clearly show that only a dilution correction has been applied internally by this FGGA. In the case of dilution only, a and $c = -0.01$, while b and $d = 0$. C_{H_2O} is of the order of 1 % in this marine environment. Accounting for volumetric dilution thus increases the reported CO_2 and CH_4 mixing ratios by about 1 %, while the correction for line broadening (based on coefficients b and d from Chen et al., 2010 and Hiller et al., 2012) is more than an order of magnitude smaller than the dilution correction. Significant biases in CO_2 and CH_4 fluxes computed from Eqs. (1) and (2) would imply that these mathematical corrections are inaccurate or insufficient at describing the cross-sensitivities between the trace gases and H_2O. The greatest relative biases are expected to occur when the magnitude of the H_2O fluctuations in the measurement cavity is large and when the trace gas fluxes are small.

The slope in mixing ratios (intercept, r^2) during Picarro (dry) vs. LGR (wet) was 1.014 (−15.5 ppm, 0.99) for $C_{CO_2\_d}$ and 0.976 (0.0113 ppm, 0.99) for $C_{CH_4\_d}$ (Picarro sampling behind a dryer). Uncertainties (relative standard deviations) of the slopes and intercepts in the fits above were ∼ 0.1 %. The calibrations of these two instruments were also crudely checked with a concentrated calibration gas mixture (8000 ppm CO_2 and 40 ppm CH_4, BOC gas). $C_{CO_2\_d}$ and $C_{CH_4\_d}$ from both instruments were within the certified uncertainty of the gas standards (5 %) so no calibration curve was applied. For the Picarro, the use of the Nafion dryer reduced the observed CO_2 mixing ratio by ∼ 0.3 % and reduced the CH_4 mixing ratio by ∼ 0.06 % when measuring the concentrated calibration gas mixture. This suggests that small amounts of CO_2 and CH_4 permeate through the Nafion dryer, qualitatively consistent with results from Welp et al. (2013).

2.3 Flux processing

Fluxes of CO_2, CH_4, and H_2O are computed using the Picarro and LGR data along with the streamline-corrected vertical wind velocity (w) from the Windmaster Pro sonic anemometer (see Yang et al., 2016 for further details about flux processing). Lag correlations between $C_{CO_2\_d}$, $C_{CH_4\_d}$ from the Picarro and LGR with w generally showed a consistent maximum covariance lag time of about 3 s. The maximum covariance lag time between H_2O and w (without a

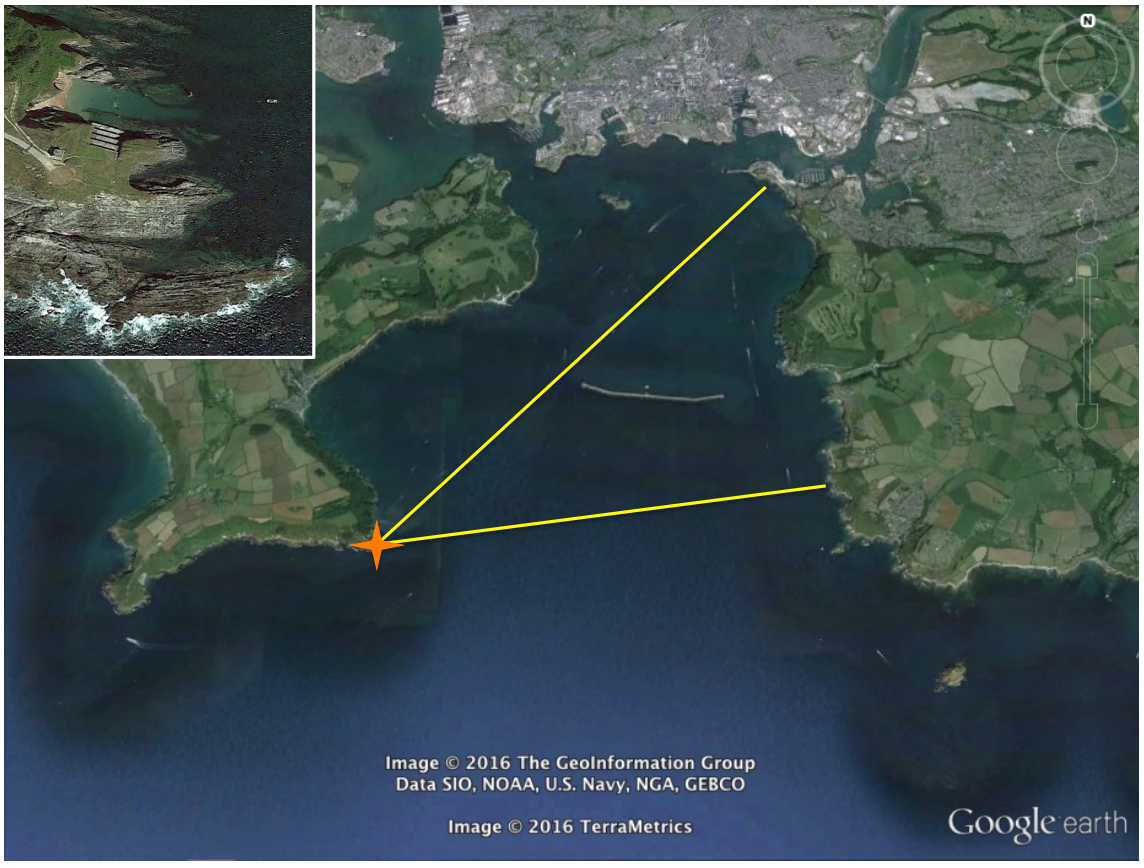

Figure 1. Location of Penlee Point Atmospheric Observatory (orange 4-point star). The yellow lines mark the air–water wind sector of 45 to 80°. The inset shows the area around the observatory (small hut in the left-centre of the image).

dryer) tended to be much longer and more variable (~ 20 s) due to severe attenuation of the high-frequency water vapour signal in the inlet tube (see Sect. 3.3).

Covariance from both instruments are computed in the same, non-overlapping 10 min intervals between lag-shifted gas-mixing ratios and w (e.g. $\overline{w'C'_{CO_2\_d}}$, $\overline{w'C'_{CH_4\_d}}$), which are multiplied by the ambient air density to yield mass concentration fluxes. Here the primes indicate fluctuations from the means while the overbar denotes temporal averaging. Because fluxes are computed from mixing ratios, an air density correction due to fluctuating temperature and pressure on the fluxes (e.g. Webb et al., 1980) should be unnecessary. The 10 min fluxes are further averaged to hourly intervals in order to reduce random noise. The relatively short averaging time of 10 min is chosen here to more easily satisfy the stationarity flux criteria in this dynamic environment. As demonstrated by Yang et al. (2016), low-frequency flux not captured by the 10 min averaging window is usually small at this site (within a few percent) and in any case the same for both analysers.

The LGR showed a positive offset in $C_{CO_2\_d}$ of ~ 15 ppm relative to the Picarro when sampling ambient air. When measuring high-purity nitrogen, the LGR CO_2 signal was also around 15 ppm initially and decayed towards zero after more than an hour (the Picarro reported CO_2, CH_4, and H_2O levels very close to zero immediately). Post-campaign tests suggest that the offset in the LGR was likely due to inaccuracy in the instrument calibration. Since the covariance flux is computed from deviations from linearly detrended mean in 10 min intervals, the positive bias in the LGR CO_2 mixing ratio should not significantly affect our flux comparison.

3 Results and discussion

Time series of CO_2 and CH_4 flux measurements during the Picarro (dry) vs. LGR (wet) period are shown in Fig. 2. For the LGR, both ambient (e.g. from C_{CO_2}) and numerically dry (e.g. from $C_{CO_2\_d}$) fluxes are shown. Considering all wind directions (137 flux hours), there is good agreement between the two instruments for dry CO_2 flux (slope = 0.99) and dry CH_4 flux (slope = 1.00). The mean (±standard error) dry CO_2 and CH_4 fluxes from the Picarro were 27.9 ± 6.4 and 0.167 ± 0.021 mmol m^{-2} day^{-1} respectively. These values agree within uncertainties with dry CO_2 and CH_4 fluxes from the LGR, which were 28.3 ± 6.7 and 0.176 ± 0.022 mmol m^{-2} day^{-1} respectively. Likewise, during the Picarro (wet) vs. LGR (wet) period, there was no sta-

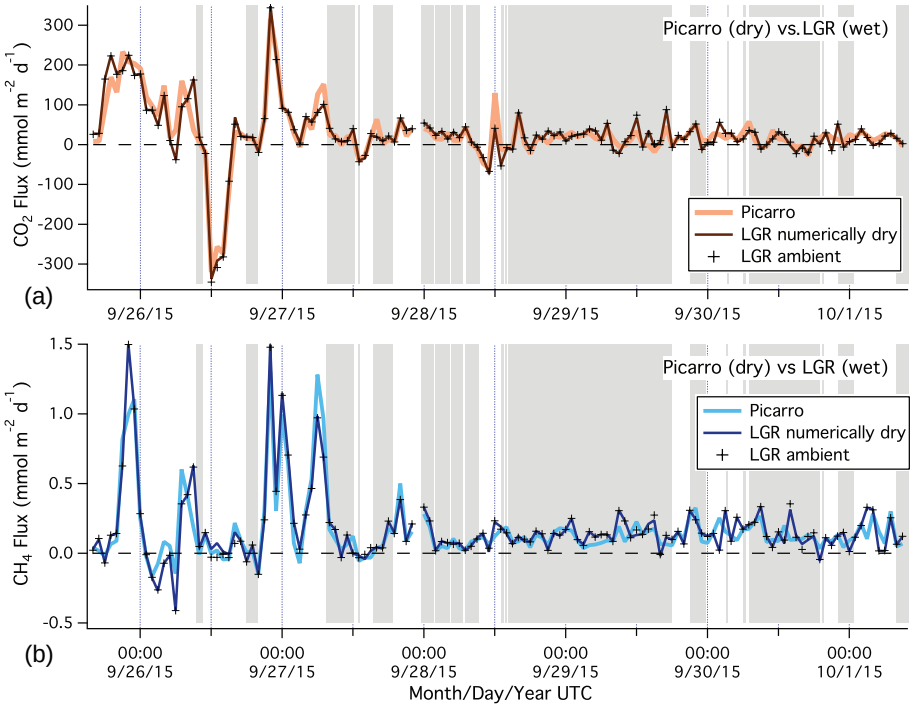

Figure 2. Time series of CO_2 (top) and CH_4 (bottom) fluxes. Picarro sampled after a dryer, while LGR sampled ambient (moist) air. "LGR ambient" indicates flux prior to the numerical H_2O correction. The shaded region indicates the wind sector between 45 and 80°.

tistically significant difference between the dry CO_2 and CH_4 fluxes from the Picarro and the LGR.

We examine the impact of the numerical H_2O correction on the CO_2 and CH_4 fluxes within a given instrument. This "intra-instrument" difference in flux, computed from numerically dry and ambient mixing ratios (i.e. $\overline{w'C'_{CH_4\_d}} - \overline{w'C'_{CH_4}}$), is plotted against the apparent H_2O flux (i.e. $\overline{w'C'_{H_2O}}$ at the optimal lag time of CH_4 / CO_2) for both the LGR and Picarro in Fig. 3. For the Picarro, these data are taken from the Picarro (wet) vs. LGR (wet) period. The slopes between the "intra-instrument" flux differences and H_2O fluxes are steeper for the Picarro than for the LGR. This is consistent with the fact that the Picarro G2311-f applies both a dilution and a line-broadening correction (Eqs. 1 and 2), while the LGR FGGA applies only the dilution correction. At typical background levels of these greenhouse gases, the expected slope of $[C_{CO_2\_d} - C_{CO_2}]$ vs. H_2O mixing ratio is ~ 0.0004 for the LGR and ~ 0.0006 for Picarro; the analogous slope in the case of CH_4 is $\sim 1.9e^{-6}$ for the LGR and $2.5e^{-6}$ for the Picarro. We see that the slopes between fluxes in Fig. 3 are essentially equal to the slopes expected between the gas-mixing ratios as a result of the numerical H_2O corrections. This is because the H_2O corrections are largely linear (i.e. coefficients b and d are close to zero).

3.1 Comparisons of air–water fluxes of CO_2 and CH_4

As indicated in Fig. 2 by the gray shading, air–water CO_2 and CH_4 fluxes tend to be much lower than terrestrial fluxes. To further evaluate the performance of these analysers at air–sea flux measurements, we limit our comparison to the sector when the wind was coming from over water only. Within the north-east quadrant, we find that the fluxes of momentum and sensible heat are reasonably consistent with air–water transfer when the wind directions were between 45 and 80° (Appendix, Figs. A2 and A3). We compare fluxes of CO_2 and CH_4 from the Picarro and LGR instruments within this wind sector in Fig. 4 (73 flux hours). Here CO_2 and CH_4 fluxes have further been filtered for stationarity following Yang et al. (2016). This removed occasional periods when the atmospheric CO_2 and CH_4 mixing ratios were highly variable (e.g. due to large horizontal transport or emissions from passing ships in the Plymouth Sound).

For both gases, fluxes from the two instruments scatter around the 1 : 1 line and differences in the mean fluxes between the two instruments are within the measurement uncertainties. During the Picarro (dry) vs. LGR (wet) period, the mean (±standard error) dry CO_2 flux was $10.7 \pm 1.8\,\mathrm{mmol\,m^{-2}\,day^{-1}}$ from the Picarro and $12.5 \pm 2.9\,\mathrm{mmol\,m^{-2}\,day^{-1}}$ from the LGR. The dry CH_4 flux was $0.110 \pm 0.009\,\mathrm{mmol\,m^{-2}\,day^{-1}}$ from the Picarro and $0.123 \pm 0.011\,\mathrm{mmol\,m^{-2}\,day^{-1}}$ from the LGR. The root mean square (rms) error between the physically dry Picarro

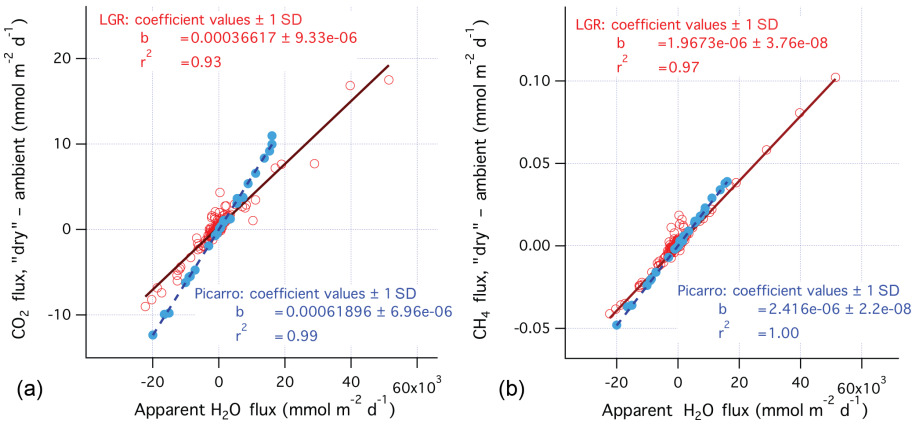

Figure 3. "Intra-instrument" difference in CO_2 (left) / CH_4 (right) fluxes computed from numerically dry and ambient CO_2 / CH_4 mixing ratios from the same instrument vs. apparent H_2O flux (latter computed at the lag time of CO_2 / CH_4). Both the LGR (red) and Picarro (blue) were directly sampling ambient air. Slopes (b) and r^2 values from the linear regressions are also shown.

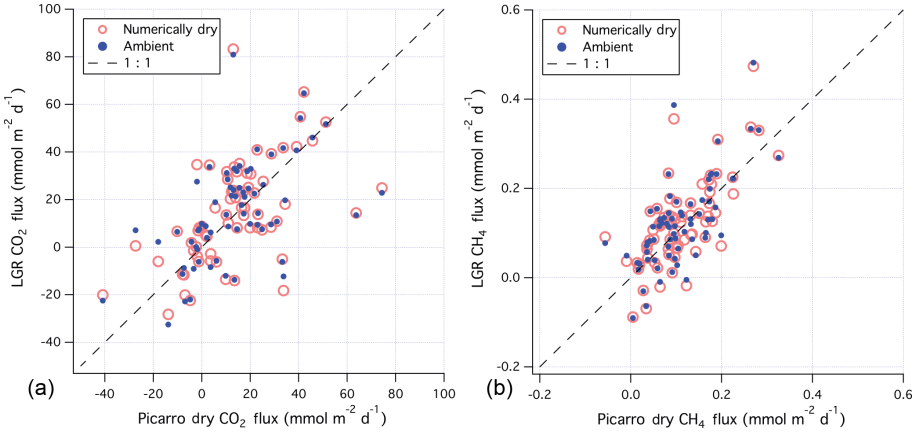

Figure 4. LGR (numerically dry and ambient) vs. Picarro (physically dry) CO_2 (left), and CH_4 (right) fluxes for the air–water wind sector of 45 to 80°. For CO_2, rms error between the two instruments is 16.1 mmol m^{-2} day^{-1} using numerically dry LGR data and 16.3 mmol m^{-2} day^{-1} using ambient LGR data. For CH_4, rms error between the two instruments is 0.063 mmol m^{-2} day^{-1} using numerically dry LGR data and 0.064 mmol m^{-2} day^{-1} using ambient LGR data.

flux and the numerically dry LGR flux (hourly average) is 16.1 mmol m^{-2} day^{-1} for CO_2 and 0.063 mmol m^{-2} day^{-1} for CH_4. The rms errors increase by only ~ 1 % when comparing the ambient LGR fluxes to the dry Picarro fluxes. Since the gas fluxes were computed using the same wind data and the two analysers were sampling the same gas stream, hourly differences in the fluxes are primarily due to noise in the two instruments, rather than by the presence of water vapour.

The effects of H_2O on the LGR fluxes were detectable but relatively small compared to the magnitude of the fluxes. This is illustrated in Fig. 5, where the differences in CO_2 and CH_4 fluxes between the LGR (numerically dry as well as ambient) and Picarro (physically dry) are plotted against the bulk air–water latent heat flux predicted from the Coupled Ocean–Atmosphere Response Experiment (COARE) model (Fairall et al., 2003). Discrepancies between the two sets of the LGR trace gas fluxes are most apparent (e.g. up to 0.04 mmol m^{-2} day^{-1} in either direction for CH_4) under conditions of high latent heat flux (i.e. highest fluctuations in H_2O mixing ratio). Qualitatively similar trends are seen when the differences in trace gas fluxes are plotted against the measured H_2O flux by the LGR (see Supplement). These results are consistent with the findings from Tuzson et al. (2010), who showed that with an earlier-generation LGR instrument, not accounting for water vapour (either physically through drying or numerically) results in a bias in the eddy covariance CH_4 flux. In our set-up, additional application of a spectral line-broadening correction (using b and d from Hiller et al., 2012) has a negligible impact on the LGR CO_2 and CH_4 fluxes.

Figure 6 shows the mean cospectra of CO_2, CH_4 (Picarro physically dry, LGR ambient, LGR numerically dry), as well as momentum when winds were from the air–water wind sec-

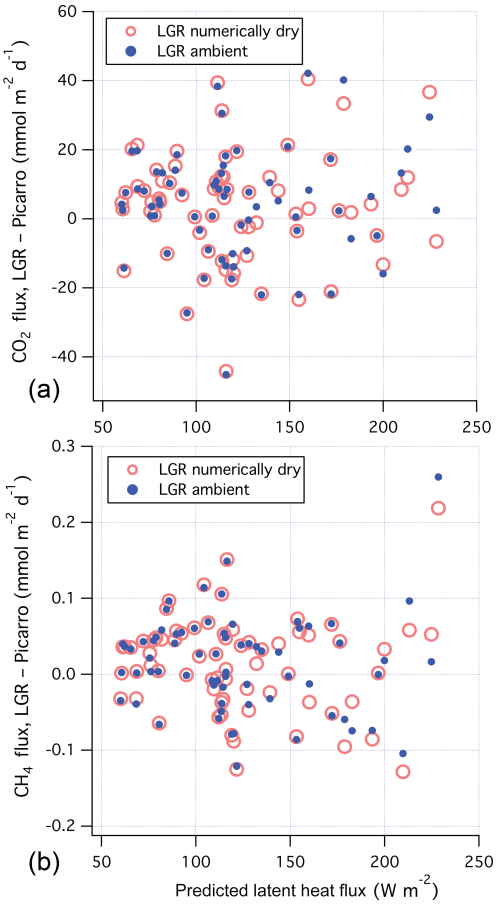

Figure 5. Differences in CO_2 (top), and CH_4 (bottom) fluxes between LGR (numerically dry as well as ambient) and Picarro (physically dry) vs. the bulk latent heat flux for the air–water wind sector of 45 to 80°. The numerical H_2O correction has the largest effect on the trace gas fluxes under conditions of high latent heat flux.

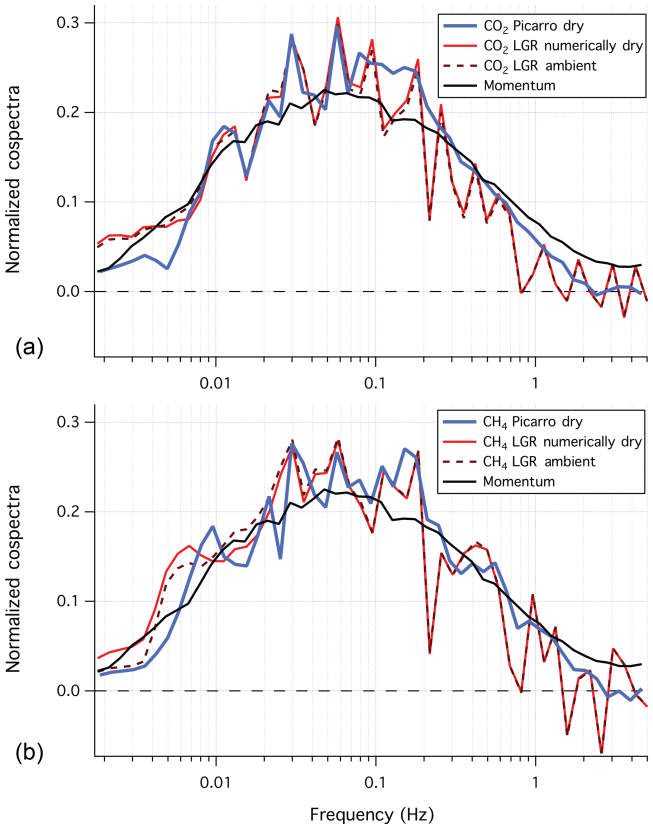

Figure 6. Mean cospectra of CO_2 (top), CH_4 (bottom) with momentum for the air–water wind sector of 45 to 80° during the Picarro (dry) vs. LGR (wet) period, normalised by the respective mean flux. Gas cospectra from the two instruments are similar in the mean and show reasonable agreement with the momentum cospectrum. Spectral similarity suggests high-frequency flux losses of ~ 6 % for CO_2 and ~ 4 % for CH_4 during this period.

tor. Each cospectrum is normalised by the respective mean flux. The gas cospectra from the two instruments have similar spectral shape to the momentum cospectrum. Numerical drying of the LGR only has a visible impact on the cospectra at low frequencies, which is likely due to the severe dampening of the H_2O flux in the main inlet tubing (Sect. 3.3). The LGR shows much more noise at frequencies above ~ 0.1 Hz, which is partly caused by the less than optimal ring-down time of the LGR analyser during our testing period (~ 8 µs instead of nominal value of ~ 12 µs). Dust and/or sea salt might have entered the LGR cavity during instrument installation, thereby reducing the ring-down time and instrument sensitivity.

3.2 Instrument noise and eddy covariance flux detection limit

Scatter (i.e. random uncertainty) in the hourly LGR flux was about 50 and 20 % higher than in the Picarro for CO_2 and CH_4 respectively. Variance spectra of $C_{CO_2\_d}$ and $C_{CH_4\_d}$ from the Picarro and LGR show much higher noise in the latter instrument (Fig. 7). These were averaged from the Picarro (dry) vs. LGR (wet) period for the air–water wind sector. Excluding the small spikes near 3 Hz (likely instrument artifacts), the mean CO_2 variance above 1 Hz (i.e. band-limited noise) was 0.0023 ppm^2 Hz^{-1} for the Picarro and 0.3 ppm^2 Hz^{-1} for the LGR. In the case of CH_4, mean variance above 1 Hz was about 0.23 ppb^2 Hz^{-1} for the Picarro and 5 ppb^2 Hz^{-1} for the LGR. Interestingly, at low frequencies the LGR variance was also greater than the Picarro (by ~ 2 times for CO_2 and ~ 60 % for CH_4). This may be partly because the LGR does not regulate the cavity temperature and pressure (1σ of about 0.005 °C and 0.16 Torr within an hour) as precisely as the Picarro (1σ of about 0.0007 °C and 0.06 Torr). Low-frequency fluctuations in H_2O, if not fully accounted for by Eqs. (1) and (2), could also cause some apparent variance in CO_2 and CH_4 dry mixing ratios.

Uncertainty, as well as detection limit, in eddy covariance gas flux depends upon variance in both the vertical wind ve-

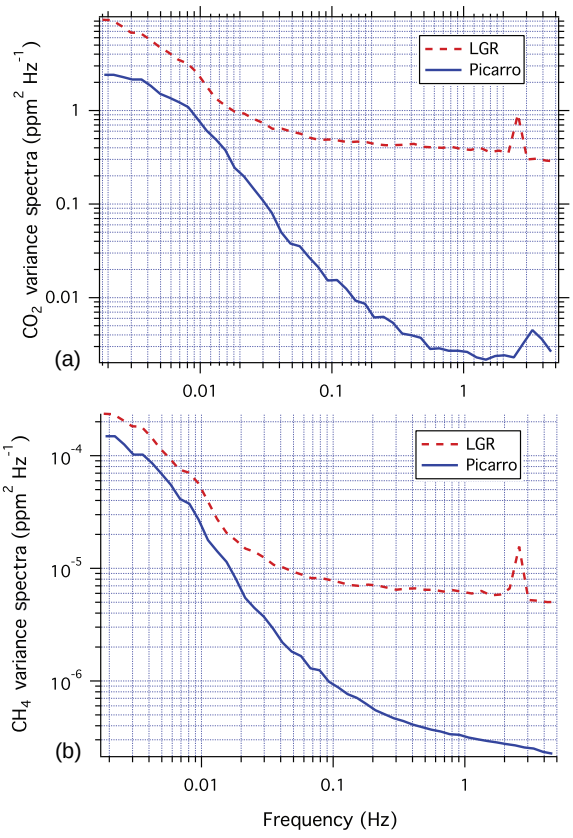

Figure 7. Mean variance spectra of dry CO_2 (top) and CH_4 (bottom) from the air–water wind sector during the Picarro (dry) vs. LGR (wet) period. The LGR shows significantly greater variance, especially at high frequencies.

locity as well as in the gas-mixing ratio. The latter is the sum of the ambient variance of the gas (estimated as the second point of the autocovariance of the mixing ratio; see Blomquist et al., 2010) and instrumental noise (estimated as the difference between the first and second points of the autocovariance). Both the Picarro and the LGR instruments are able to resolve rapid ambient fluctuations in atmospheric CO_2 and CH_4. For example, ambient variance in $C_{CH_4\_d}$ (i.e. without instrument noise) from the two instruments agree almost exactly (slope = 1.00; $r^2 = 0.96$).

Based on earlier measurements at PPAO, Yang et al. (2016) estimated a CH_4 flux detection limit of 0.02 mmol m^{-2} day^{-1} (hourly average) for the Picarro G2311-f at a wind speed of 10 m s^{-1}. This was quantified using two different methods that yielded largely comparable results: a theoretically based method on instrument noise and ambient variance (Blomquist et al., 2014) and an empirically based method on scatter in $\overline{w'C'_{CH_4}}$ at an implausible lag time (e.g. 300 s). Applying the same methods to CO_2 here results in a flux detection limit between 2.2 mmol m^{-2} day^{-1} (theoretical) and 4 mmol m^{-2} day^{-1} (empirical) for the G2311-f. At a wind speed of 10 m s^{-1} and in a neutral atmosphere, Blomquist et al. (2014) computed a CO_2 flux detection limit of 1.3 mmol m^{-2} day^{-1} (hourly average) for a prototype Picarro analyser G1301-f. The instrument used by Blomquist et al. (2014) only measures CO_2 and thus has a lower noise level of 700 ppb^2 Hz^{-1} (see their Fig. 6) than the Picarro we deployed at PPAO. The high-frequency noise of dry CO_2 and CH_4 in the Picarro are comparable with and without the Nafion dryer. Thus, we do not expect the dryer to cause a significant difference in the Picarro detection limits.

Following Blomquist et al. (2014), we theoretically estimate the flux detection limits for the LGR FGGA using the band-limited noise shown in Fig. 7 and ambient variance from periods of very low variability (100 and 0.04 ppb^2 for CO_2 and CH_4 respectively). At a wind speed of 10 m s^{-1} and in a neutral atmosphere, we estimate a flux detection limit of 13.5 mmol m^{-2} day^{-1} for CO_2 and 0.060 mmol m^{-2} day^{-1} for CH_4 (hourly average). We also examined an earlier measurement period when the LGR had the optimal sensitivity (ring-down time of 12 µs), with band-limited noise of 0.11 ppm^2 Hz^{-1} for CO_2 and 3.7 ppb^2 Hz^{-1} for CH_4. Coupling these noise levels to the ambient variability above, at the same environmental conditions, we estimate a best case hourly flux detection limit for the LGR of 8.2 mmol m^{-2} day^{-1} for CO_2 and 0.053 mmol m^{-2} day^{-1} for CH_4 (see Table 1 for summary). In the case of CO_2, the LGR flux detections limits are of the same magnitude as those from the LI-COR LI7200 with a dryer (as estimated by Blomquist et al., 2014).

It is useful to put these flux detection limits into the context of regions of the ocean and times of year that are favourable for future process-level studies with direct flux measurements (e.g. research cruises that aim to improve our understanding of the gas transfer velocity). For illustrative purposes, we compare the CO_2 flux detection limits with the estimated global air–sea CO_2 flux maps from the National Oceanographic and Atmospheric Administration's Pacific Marine Environmental Laboratory (http://www.pmel.noaa.gov/co2/story/Surface+_CO2+_Flux+_maps; Feely et al., 2006; Sabine et al., 2008, 2009; Park et al., 2010). Four monthly maps from 2015 to 2016 (4° resolution) are chosen to capture seasonal variations: March, June, September, and December. Globally, the absolute value of the estimated monthly mean CO_2 flux exceeds 2 mmol m^{-2} day^{-1} (hourly flux detection limit of the Picarro) in roughly 39–44 % of the oceans (highest in March) and exceeds 8 mmol m^{-2} day^{-1} (detection limit of the LGR) in 2–6 % of the oceans (highest in December). The North Atlantic and North Pacific, southeastern Pacific, and the Southern Ocean are not surprisingly amongst regions favourable for eddy covariance CO_2 flux measurements. When estimated fluxes are comparable or below the hourly flux detection limit, further averaging of the eddy covariance measurements (temporally or in bins of wind speed, etc.) will likely be necessary to extract statistically meaningful results (as random uncertainty in flux decreases with increasing number of independent hourly mea-

Table 1. Performance of the Picarro G2311-f and LGR FGGA at measuring CO_2 and CH_4 fluxes by eddy covariance. Precision refers to observed noise at 10 Hz. Band-limited noise is averaged between 1 and 5 Hz from the mean variance spectra. Flux detection limit is estimated at a wind speed of 10 m s^{-1} in a neutral atmosphere (hourly average). The FGGA band-limited noise and detection limit correspond to when the ring-down time was optimal and the instrument sensitivity at its highest.

CO_2	Precision (10 Hz)	Band-limited noise	Flux detection limit
	[ppm]	[ppm^2 Hz^{-1}]	[mmol m^{-2} day^{-1}]
Picarro G2311-f	0.15	0.0023	2
LGR FGGA	1.4	0.11	8
CH_4	Precision (10 Hz)	Band-limited noise	Flux detection limit
	[ppb]	[ppb^2 Hz^{-1}]	[mmol m^{-2} day^{-1}]
Picarro G2311-f	1.1	0.23	0.02
LGR FGGA	5.5	3.7	0.05

surements, N, by the relationship of $N^{-0.5}$). For example, if the hourly fluxes are binned to 6 h intervals the percentage of exceedance as described above may improve to 65 and 24 % for the Picarro and LGR respectively (averaged across all seasons).

The predicted open ocean emission of CH_4 is of the order of 0.01 mmol m^{-2} day^{-1} (Forster et al., 2009). Thus, further binning of hourly eddy covariance measurements (e.g. to 6 h or daily intervals) would likely be needed to better resolve CH_4 fluxes. The signal-to-noise ratio in the eddy covariance CH_4 flux measurement should be improved near the coast (e.g. Bange, 2006) and in the Arctic (e.g. Shakhova et al., 2010), where surface saturations and hence emissions of CH_4 are likely greater. Combining data from a floating chamber with a turbulent diffusivity model, Kitidis et al. (2007) estimated a CH_4 emission of 0.06 to 0.17 mmol m^{-2} day^{-1} in a large coastal embayment. CH_4 flux of a similar magnitude has been measured here at PPAO (this paper and Yang et al., 2016). Aircraft observations suggest CH_4 emissions over 0.1 mmol m^{-2} day^{-1} from the partially ice-covered Arctic (Kort et al., 2012), which are above the flux detection limits of both analysers.

We did not evaluate the effect of motion on these analysers. During the High Wind Gas Exchange Study (HiWinGS) cruise in 2013 (Yang et al., 2014b), a Picarro G1301-f was deployed with a Nafion dryer along with a second generation model from Picarro (G2301-f) which was not sampling after a dryer. In moderate seas, the two instruments yielded similar CO_2 fluxes, implying that the numerical H_2O correction in G2301-f is reasonable. However, the different sensitivities of these two models to the ship's motion in high seas complicated these flux comparisons (B. Blomquist, personal communication, 2016). Side-by-side shipboard deployments of the Picarro and LGR are required to provide a more conclusive verdict on the optimal flux analyser for air–sea flux measurements.

3.3 High-frequency flux loss

Based on measurements of dimethylsulfide (DMS) flux, Blomquist et al. (2010) and Yang et al. (2011) reported high-frequency flux attenuations to be of the order of 5 % using a long inlet and the same type of Nafion dryer as used here for the Picarro. CO_2 and CH_4 are less polar (i.e. less "sticky") gases than DMS so we expect their flux losses in the dryer to be comparable or less. CO_2 and CH_4 flux attenuation by the tubing itself should be a few percent at most given the fully turbulent flow used in our study (Lenschow and Raupach, 1991; Ibrom et al., 2007). Below we quantify the high-frequency attenuations in the CO_2 and CH_4 fluxes from the Picarro (with and without a dryer) and the LGR (without a dryer).

The effect of the Nafion dryer on the Picarro instrument response is clearly illustrated in Fig. 8. Here we made rapid, stepwise reductions in the flow rates of the concentrated CO_2 and CH_4 gas standard (here controlled by a digital mass flow controller, EL-FLOW, Bronkhorst), which was teed into the gas inlet with and without the dryer. For ease of comparison, we normalise the dry CO_2 and CH_4 such that the signals decrease from one to zero. Without the dryer, the observed response time (defined as the time needed for the signal to fall to $1/e$ of the initial value) was about 0.2 s. This is 0.1 s longer than the expected instrumental response time, likely in part due to the finite time response of the mass flow controller (settling time of 0.1–0.2 s). With the dryer, the signal drop-off was noticeably slower and the observed response time increased to about 0.5 s. The response time for CO_2 appears to be very slightly longer than for CH_4 in the presence of the dryer, as might be expected from the greater permeation (i.e. breakthrough) of CO_2 through the Nafion membranes compared to CH_4. Knowing the instrument response time allows us to estimate the high-frequency flux loss using a filter function (e.g. Bariteau et al., 2010; Yang et al., 2014a; Blomquist et al., 2014). At a response time of 0.3 s with the dryer (accounting for the settling time of the mass flow con-

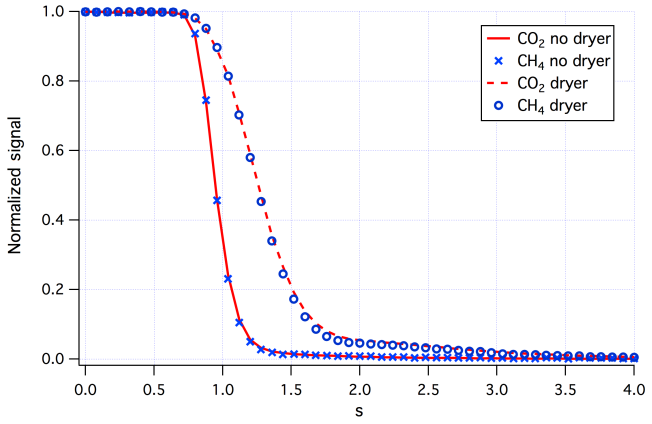

Figure 8. Fall offs in the Picarro dry CO_2 and CH_4 signals shortly after reductions in the calibration gas flow rate. The use of a Nafion dryer increases the observed response time by about 0.3 s.

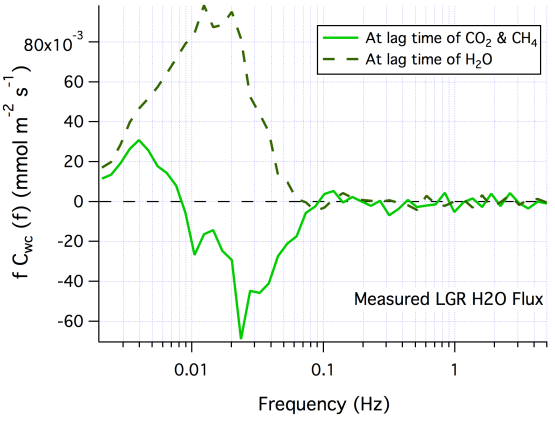

Figure 9. Mean cospectra of LGR H_2O flux for the air–water wind sector, computed at the optimal lag time of CO_2 / CH_4 (3 s) and the optimal lag time of H_2O (~ 20 s). The much longer lag time of H_2O is due to severe high-frequency attenuation of H_2O in the inlet tube (e.g. no flux signal above ~ 0.1 Hz). Even at the optimal lag time, measured H_2O flux is only about 10 % of the predicted latent heat flux (mean of 120 W m^{-2}).

troller), the predicted flux loss in the Picarro averaged over the Picarro (dry) vs. LGR (wet) period (mean wind speed of 10 m s^{-1}) is 10 %. Without the dryer the predicted flux loss is reduced to only ~ 4 % at this wind speed.

Compared to the momentum cospectrum, the Picarro CO_2 and CH_4 cospectra are noticeably attenuated above the frequency of about 1 Hz (Fig. 6). High-frequency loss in the gas fluxes can also be estimated by similarity scaling with respect to another variable (often sensible heat). Air–water sensible heat flux varied in sign between day and night during this period, resulting in a very noisy mean cospectrum. Thus, we use momentum cospectrum for comparison instead. We convert the cospectra of gases and momentum to ogive (Oncley, 1989), or the cumulative sum of the cospectrum from low to high frequency. Following the method outlined by Spirig et al. (2005), from the ogive, we estimate that the mean loss of flux is about 6 % for CO_2 and 4 % for CH_4, somewhat less than the filter function estimates above.

For the LGR, the large volume of the cavity cell was the principal limitation to the instrument response time, so it was likely the main cause for flux attenuation. Judging from the cospectra, the CO_2 and CH_4 flux attenuation in the LGR is comparable to the Picarro with a Nafion dryer. We note that the flow rate through the LGR can be increased substantially (by approximately a factor of seven) relative to the set-up here by adjusting the external scroll pump and using an inlet tube with a larger inner diameter. A faster airflow through the LGR cavity (e.g. flushing time of 0.1 s) would reduce the estimated flux loss in the LGR analyser to only a few percent; it likely would not significantly improve the instrument noise or flux detection limit, however.

Unlike CO_2 and CH_4, fluctuations in water vapour are severely attenuated in our main inlet tube (similar to Ibrom et al., 2007). This is because the polar H_2O is a much "stickier" gas than CO_2 and CH_4 and tends to absorb onto the wall of the tubing. Figure 9 shows the mean cospectrum of LGR H_2O, which was computed at the maximum covariance lag time of CO_2 / CH_4 (3 s) as well as at the optimal lag time for H_2O (~ 20 s). H_2O cospectrum computed at a lag time of 3 s is positive at the lowest frequencies and negative between about 0.01 and 0.1 Hz (resulting in mean apparent H_2O flux near zero). In reality, the calculated bulk latent heat flux was always positive during this period, averaging 120 W m^{-2} (range of 60–230 W m^{-2}).

Computed at the optimal lag time of ~ 20 s, H_2O cospectrum from the LGR is positive at frequencies below ~ 0.1 Hz. Above 0.1 Hz the measured H_2O flux is essentially zero (i.e. flux completely attenuated). Comparison with the bulk latent heat flux suggests that only up to 20 % of the H_2O flux is still detectable after going through ~ 18 m of inlet tubing (see Supplement). H_2O flux from the Picarro without the Nafion dryer yielded similar results, confirming the importance of the sample tubing at attenuating the H_2O flux. In our set-up, H_2O flux attenuation might be particularly severe because the tubing we used had been constantly exposed to marine air for 1.5 years, resulting in accumulation of hygroscopic sea salt particles on the tubing wall. In a case of a shorter, cleaner inlet tubing, dampening of H_2O fluctuations in the tubing should be somewhat reduced and the impact of H_2O on CO_2 and CH_4 fluxes may be greater. Forgoing a physical drier would increase the reliance on the numerical H_2O correction for accurate determination of CO_2 and CH_4 fluxes.

4 Conclusions

In this paper we compared the performance of the Picarro G2311-f (with and without a Nafion dryer) and the Los Gatos Research FGGA (without a dryer) at eddy covariance measurements of air–water CO_2 and CH_4 fluxes. Within measurement uncertainties, dry CO_2 and CH_4 fluxes from these two analysers agree. For winds over the Plymouth Sound, air–water CO_2 and CH_4 fluxes averaged about 12 and 0.12 mmol m^{-2} day^{-1} respectively. In our closed-path set-up with a long inlet tube, the numerical corrections of CO_2 and CH_4 mixing ratios based on concurrently measured H_2O appeared to be reasonably effective for both instruments. Numerically dry CO_2 and CH_4 fluxes from the LGR agree within uncertainties in the mean with results from the Picarro after physical removal of H_2O using a Nafion dryer. Coupling the LGR to a dryer, which we did not test, may have slightly improved the flux precision. The addition of a dryer would reduce the reliance on the instrumental numerical correction for H_2O, but could increase flux attenuation and potentially cause a small bias in the mean CO_2 and CH_4 mixing ratios. Flux attenuation in the Picarro (likely occurring primarily within the dryer) was within 10 % for both CO_2 and CH_4. Similar flux losses were observed for the LGR without a dryer in our set-up (likely occurring primarily within the large cavity), which could be reduced by increasing the airflow through the instrument. In contrast to CO_2 and CH_4, H_2O fluctuations were severely dampened in our inlet tubing, resulting in $\geq$ 80 % loss of the latent heat flux. Compared to the LGR, the Picarro demonstrated significantly lower noise levels, so flux detection limits were also lower (Table 1). These estimates help to advise us on the choices of location and timing for future process-level studies on air–sea CO_2 and CH_4 transfer.

5 Data availability

Processed hourly eddy covariance fluxes can be found in the Supplement of this paper. Raw data files at 10 Hz are very large (tens of gigabytes) and currently not archived in an online database. Please contact us directly if you are interested in the raw data and we would be very happy to share them.

Appendix A: Selection of wind sector for air–water transfer

The PPAO site is exposed to marine air over a wide wind sector from about 30 to 250° (Fig. 1). Wind was mostly from the north-east during this period of instrument intercomparison (Fig. A1). Within this quadrant, we find that the fluxes of momentum (Fig. A2) as well as sensible heat (Fig. A3) are reasonably consistent with air–water transfer when the wind directions were from 45–80°. As shown by the inset in Fig. 1, the distance between PPAO and the water's edge is about 20–30 m towards the north-east. North of a wind direction of 45°, the flux footprint begins to overlap with land (Mount Edgcumbe Country Park). Immediately south of 80°, the longer foreshore in front of PPAO likely affects the flux footprint and increases the effect of airflow distortion on the measured wind speed. The 10 m neutral drag coefficient is computed as $C_{D10N} = u_*/U_{10N}$. Here u_* is the friction velocity measured by eddy covariance and the 10 m neutral wind speed U_{10N} is determined using Businger–Dyer relationships (Businger, 1988) from the wind speed and air temperature at PPAO, tidal-dependent sampling height, and sea-surface temperature (SST) from the L4 mooring station ($\sim$ 6 km south of PPAO). Within 45–80°, C_{D10N} increases with wind speed, as expected for air–water transfer. Values of C_{D10N} are, however, about $\sim$ 20 % lower than parameterisations for open water in the mean (e.g. COARE model version 3.5, Edson et al., 2013; Smith, 1980), possibly due to flow distortion of the mean wind speed or a residual bias in the Windmaster Pro wind measurement (see Yang et al., 2016 for more details).

Sensible heat flux was computed from the sonic temperature and further corrected for the bulk latent heat contribution (Schotanus et al., 1983). It shows a surprisingly good agreement (slope = 0.98 and $r^2 = 0.87$) with sensible heat flux estimated with the COARE model (Fairall et al., 2003) using air temperature and wind speed at PPAO as well as SST from L4. This close agreement despite the relatively long distance between the flux footprint and the mooring station was possibly due to fair weather in September 2015 and minimal riverine influence in the flux footprint (i.e. negligible spatial gradient in SST). Sensible heat flux was on average positive at night and negative during the day, primarily due to diel variability in air temperature. In spite of this variation, the atmosphere was near neutral during this measurement period as a result of the relatively strong winds (mean of 10 m s^{-1}). The predicted atmospheric stability parameter z/L varied from about -0.20 at night to 0.05 during the day. Thus, we do not expect the flux footprint to extend beyond the 5–6 km fetch of water to the opposite side of the Plymouth Sound (as could happen during periods of extreme stability). Note that a flux footprint extending over land would cause momentum and sensible heat fluxes to grossly deviate from the predicted bulk air–sea fluxes, which was not observed.

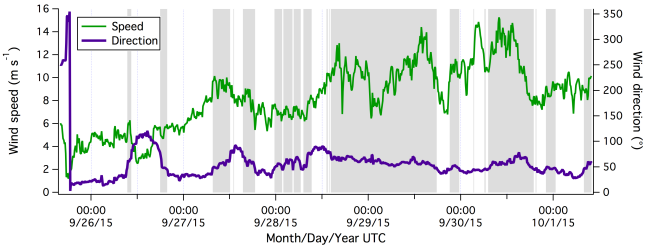

Figure A1. Time series of wind speed and direction during the Picarro (dry) vs. LGR (wet) period. The shaded region indicates the wind sector between 45 and 80°, which we consider to be representative of air–water transfer.

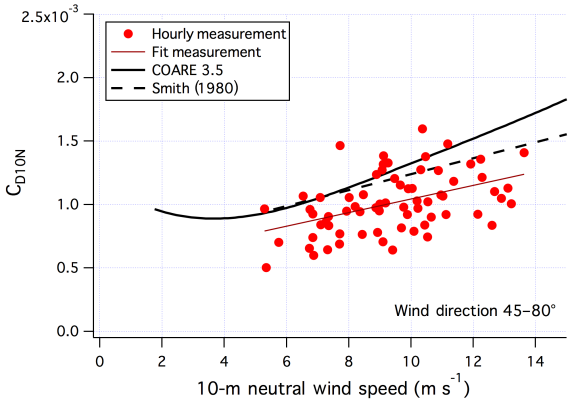

Figure A2. 10 m neutral drag coefficient vs. 10 m neutral wind speed for the air–water wind sector.

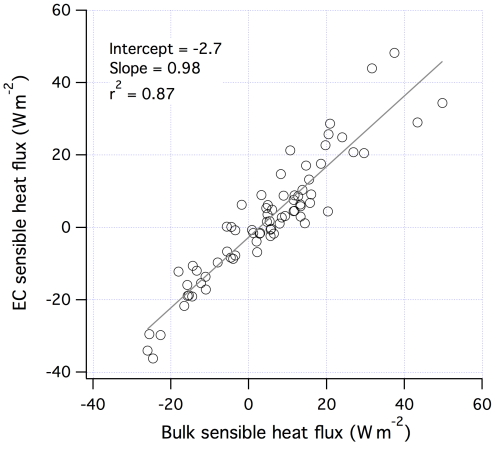

Figure A3. Measured vs. predicted sensible heat flux for the air–water wind sector.

The Supplement related to this article is available online at doi:10.5194/amt-9-5509-2016-supplement.

Acknowledgements. This work is a contribution to the ACSIS (The North Atlantic Climate System Integrated Study) and ORCHESTRA (Ocean Regulation of Climate through Heat and Carbon Sequestration and Transports) project funded by the Natural Environment Research Council, UK. Trinity House (http://www.trinityhouse.co.uk/) owns the Penlee site and has kindly agreed to rent the building to PML so that instrumentation can be protected from the elements. We are able to access the site thanks to the cooperation of Mount Edgcumbe Estate (http://www.mountedgcumbe.gov.uk/). We thank A. J. Watson (University of Exeter), P. D. Nightingale and T. J. Smyth (PML) for support, as well as B. W. Blomquist (US National Oceanographic and Atmospheric Administration) for helpful comments and suggestions. The participation of D. Parenkat Mony was funded by the Partnership for Observation of the Global Oceans (POGO) programme. This is PPAO publication NO. 3.

Edited by: C. Brümmer
Reviewed by: S. Landwehr and B. Butterworth

References

Bange, H. W.: Nitrous oxide and methane in European coastal waters, Estuar. Coast. Shelf Sci., 70, 361–374, 2006.

Bariteau, L., Helmig, D., Fairall, C. W., Hare, J. E., Hueber, J., and Lang, E. K.: Determination of oceanic ozone deposition by ship-borne eddy covariance flux measurements, Atmos. Meas. Tech., 3, 441–455, doi:10.5194/amt-3-441-2010, 2010.

Blomquist, B. W., Huebert, B. J., Fairall, C. W., and Faloona, I. C.: Determining the sea-air flux of dimethylsulfide by eddy correlation using mass spectrometry, Atmos. Meas. Tech., 3, 1–20, doi:10.5194/amt-3-1-2010, 2010.

Blomquist, B. W., Huebert, B. J., Fairall, C. W., Bariteau, L., Edson, J. B., Hare, J. E., and McGillis, W. R.: Advances in Air-Sea CO_2 Flux Measurement by Eddy Correlation, Bound.-Lay. Meteorol., 152, 245–276, doi:10.1007/s10546-014-9926-2, 2014.

Businger, J. A.: A note on the Businger–Dyer profiles. Bound.-Lay. Meteorol., 42, 145–151, doi:10.1007/978-94-009-2935-7_11, 1988.

Chen, H., Winderlich, J., Gerbig, C., Hoefer, A., Rella, C. W., Crosson, E. R., Van Pelt, A. D., Steinbach, J., Kolle, O., Beck, V., Daube, B. C., Gottlieb, E. W., Chow, V. Y., Santoni, G. W., and Wofsy, S. C.: High-accuracy continuous airborne measurements of greenhouse gases (CO_2 and CH_4) using the cavity ring-down spectroscopy (CRDS) technique, Atmos. Meas. Tech., 3, 375–386, doi:10.5194/amt-3-375-2010, 2010.

Edson, J. B., Fairall, C. W., Bariteau, L., Zappa, C. J., Cifuentes-Lorenzen, A., McGillis, W. R., Pezoa, S., Hare, J. E., and Helmig, D.: Direct covariance measurement of CO_2 gas transfer velocity during the 2008 Southern Ocean Gas Exchange Experiment: wind speed dependency, J. Geophys. Res.-Oceans, 116, C00F10, doi:10.1029/2011JC007022, 2011.

Edson, J. B., Jampana, V., Weller, R. A., Bigorre, S. P., Plueddemann, A. J., Fairall, C. W., Miller, S. D., Mahrt, L., Vickers, D., and Hersbach H.: On the exchange of momentum over the open ocean, J. Phys. Oceanogr., 43, 1589–1610, doi:10.1175/JPO-D-12-0173.1, 2013.

Fairall, C. W., Bradley, E. F., Hare, J. E., Grachev, A. A., and Edson, J. B.: Bulk parameterization of air-sea fluxes: updates and verification for the COARE algorithm, J. Clim., 16, 571–591, 2003.

Feely, R. A., Takahashi, T., Wanninkhof, R., McPhaden, M. J., Cosca, C. E., Sutherland, S. C., and Carr, M.-E.: Decadal variability of the air-sea CO_2 fluxes in the equatorial Pacific Ocean, J. Geophys. Res., 111, C08S90, doi:10.1029/2005JC003129, 2006.

Forster, G. L., Upstill-Goddard, R. C., Gist, N., Robinson, R., Uher, G., and Woodward, E. M. S.: Nitrous oxide and methane in the Atlantic Ocean between 501N and 521S: Latitudinal distribution and sea-to-air flux, Deep-Sea Res. Pt. II, 56, 964–976, doi:10.1016/j.dsr2.2008.12.002, 2009.

Hiller, R. V., Zellweger, C., Knohl, A., and Eugster, W.: Flux correction for closed-path laser spectrometers without internal water vapor measurements, Atmos. Meas. Tech. Discuss., 5, 351–384, doi:10.5194/amtd-5-351-2012, 2012.

Ibrom, A., Dellwik, E., Flyvbjerg, H., Jensen, N. O., and Pilegaard, K.: Strong low-pass filtering effects on water vapour flux measurements with closed-path eddy correlation systems, Agr. Forest Meteorol., 147, 140–156, doi:10.1016/j.agrformet.2007.07.007, 2007.

Kitidis, V., Tizzard, L., Uher, G., Judd, A., Upstill-Goddard, R. C., Head, I. M., Gray, N. D., Taylor, G., Duran, R., Diez, R., Iglesias, J., and Garcia-Gil, S.: The biogeochemical cycling of methane in Ria de Vigo, NW Spain: Sediment processing and sea-air exchange, J. Mar. Syst., 66, 258–271, 2007.

Kondo, F., Ono, K., Mano, M., Miyata, A., and Tsukamoto, O.: Experimental evaluation of water vapour cross-sensitivity for accurate eddy covariance measurement of CO_2 flux using open-path CO_2 / H_2O gas analysers, Tellus B, 66, 23803, doi:10.3402/tellusb.v66.23803, 2014.

Kort, E. A., Wofsy, S. C., Daube, B. C., Diao, M., Elkins, J. W., Gao, R. S., Hintsa, E. J., Hurst, D. F., Jimenez, R., Moore, F. L., Spackman, J. R., and Zondlo, M. A.: Atmospheric observations of Arctic Ocean methane emissions up to 82 degrees north, Nat. Geosci., 5, 318–321, doi:10.1038/ngeo1452, 2012.

Landwehr, S., Miller, S. D., Smith, M. J., Saltzman, E. S., and Ward, B.: Analysis of the PKT correction for direct CO_2 flux measurements over the ocean, Atmos. Chem. Phys., 14, 3361–3372, doi:10.5194/acp-14-3361-2014, 2014.

Lenschow, D. and Raupach, M.: The attenuation of fluctuations in scalar concentrations through sampling tubes, J. Geophys. Res., 96, 15259–15268, 1991.

Miller, S. D., Marandino, C., and Saltzman, E. S.: Ship-based measurement of air-sea CO_2 exchange by eddy covariance, J. Geophys. Res., 115, D02304, doi:10.1029/2009JD012193, 2010.

O'Keefe, A. and Deacon, D. A. G.: Cavity ring-down optical spectrometer for absorption measurements using pulsed laser sources, Rev. Sci. Inst., 59, 2544–2551, 1988.

O'Keefe, A., Scherer, J. J., and Paul, J. B.: CW integrated cavity output spectroscopy, Chem. Phys. Lett., 307, 343–349, 1999.

Oncley, S. P.: Flux Parameterisation Techniques in the Atmospheric Surface Layer, PhD thesis, 202 pp., Univ. of California, Irvine, 1989.

Peltola, O., Hensen, A., Helfter, C., Belelli Marchesini, L., Bosveld, F. C., van den Bulk, W. C. M., Elbers, J. A., Haapanala, S., Holst, J., Laurila, T., Lindroth, A., Nemitz, E., Röckmann, T., Vermeulen, A. T., and Mammarella, I.: Evaluating the performance of commonly used gas analysers for methane eddy covariance flux measurements: the InGOS inter-comparison field experiment, Biogeosciences, 11, 3163–3186, doi:10.5194/bg-11-3163-2014, 2014.

Park, G.-H., Wanninkhof, R., Doney, S. C., Takahashi, T., Lee, K., Feely, R. A., Sabine, C., Triñanes, J., and Lima, I.: Variability of global air-sea CO_2 fluxes over the last three decades, Tellus, 62B, 352–368, doi:10.1111/j.1600-0889.2010.00498.x, 2010.

Prytherch, J., Yelland, M. J., Pascal, R. W., Moat, B. I., Skjelvan, I., and Neill, C. C.: Direct measurements of the CO_2 flux over the ocean: development of a novel method, Geophys. Res. Lett., 37, L03607, doi:10.1029/2009GL041482, 2010.

Prytherch, J., Yelland, M. J., Brooks, I. M., Tupman, D. J., Pascal, R. W., Moat, B. I., and Norris, S. J.: Motion-correlated flow distortion and wave-induced biases in air-sea flux measurements from ships, Atmos. Chem. Phys., 15, 10619–10629, doi:10.5194/acp-15-10619-2015, 2015.

Rella, C. W.: Accurate Greenhouse Gas Measurements in Humid Gas Streams Using the Picarro G1301 Carbon Dioxide/Methane/Water Vapor Gas Analyzer, Tech. rep., 2010.

Sabine, C. L., Feely, R. A., Wanninkhof, R., and Takahashi, T.: The global ocean carbon cycle, in: State of the Climate in 2007, edited by: Levinson, D. H. and Lawrimore, J. H., B. Am. Meteorol. Soc., 89, S52–S56, 2008.

Sabine, C. L., Feely, R. A., Wanninkhof, R., and Takahashi, T.: The global ocean carbon cycle, in: State of the Climate in 2008, edited by: Levinson, D. H. and Lawrimore, J. H., B. Am. Meteorol. Soc., 90, S65–S68, 2009.

Schotanus, P., Nieuwstadt, F. T. M., and de Bruin, H. A. R.: Temperature Measurement with a Sonic Anemometer and its Application to Heat and Moisture Fluxes, Bound.-Lay. Meteorol., 26, 81–93, 1983.

Shakhova, N., Semiletov, I., Salyuk, A., Yusupov, V., Kosmach, D., and Gustafsson, O.: Extensive methane venting to the atmosphere from sediments of the east Siberian Arctic shelf, Science, 327, 1246–1250, 2010.

Smith, S.: Wind stress and heat flux over the ocean in gale force winds, J. Phys. Oceanogr., 10, 709–726, 1980.

Spirig, C., Neftel, A., Ammann, C., Dommen, J., Grabmer, W., Thielmann, A., Schaub, A., Beauchamp, J., Wisthaler, A., and Hansel, A.: Eddy covariance flux measurements of biogenic VOCs during ECHO 2003 using proton transfer reaction mass spectrometry, Atmos. Chem. Phys., 5, 465–481, doi:10.5194/acp-5-465-2005, 2005.

Tuzson, B., Hiller, R. V., Zeyer, K., Eugster, W., Neftel, A., Ammann, C., and Emmenegger, L.: Field intercomparison of two optical analyzers for CH_4 eddy covariance flux measurements, Atmos. Meas. Tech., 3, 1519–1531, doi:10.5194/amt-3-1519-2010, 2010.

Webb, E. K., Pearman, G. I., and Leuning, R.: Correction of flux measurements for density effects due to heat and water vapour transfer, Q. J. Roy. Meteor. Soc., 106, 85–100, 1980.

Welp, L. R., Keeling, R. F., Weiss, R. F., Paplawsky, W., and Heckman, S.: Design and performance of a Nafion dryer for continuous operation at CO_2 and CH_4 air monitoring sites, Atmos. Meas. Tech., 6, 1217–1226, doi:10.5194/amt-6-1217-2013, 2013.

Yang, M., Blomquist, B. W., Fairall, C. W., Archer, S. D., and Huebert, B. J.: Air-sea exchange of dimethylsulfide in the Southern Ocean: measurements from SO GasEx compared to temperate and tropical regions, J. Geophys. Res., 116, C00F05, doi:10.1029/2010JC006526, 2011.

Yang, M., Beale, R., Liss, P., Johnson, M., Blomquist, B., and Nightingale, P.: Air-sea fluxes of oxygenated volatile organic compounds across the Atlantic Ocean, Atmos. Chem. Phys., 14, 7499–7517, doi:10.5194/acp-14-7499-2014, 2014a.

Yang, M., Blomquist, B. W., and Nightingale P. D.: Air-sea exchange of methanol and acetone during HiWinGS: Estimation of air phase, water phase gas transfer velocities, J. Geophys. Res.-Oceans, 119, 7308–7323, doi:10.1002/2014JC010227, 2014b.

Yang, M., Bell, T. G., Hopkins, F. E., Kitidis, V., Cazenave, P. W., Nightingale, P. D., Yelland, M. J., Pascal, R. W., Prytherch, J., Brooks, I. M., and Smyth, T. J.: Air-sea fluxes of CO_2 and CH_4 from the Penlee Point Atmospheric Observatory on the southwest coast of the UK, Atmos. Chem. Phys., 16, 5745–5761, doi:10.5194/acp-16-5745-2016, 2016.